A New, Near-Coherent Detector Configuration for UWB Impulse Radio

Tamás Krébesz[†] and Géza Kolumbán[‡]

†‡Dept. of Measurement and Information Systems, Budapest University of Technology and Economics
H-1521 Budapest Pf. 91, Hungary
Email: {krebesz,kolumban}@mit.bme.hu

Abstract—Since radio channels available have been assigned to traditional narrowband communication systems the only solution to establish new radio communication links is the frequency reuse. This has to be achieved without causing interference in the conventional radio systems. Ultra WideBand (UWB) radio uses extremely wideband wavelets to decrease the Power Spectral Density (psd) of radiated signal. In this paper a new demodulation technique called near-coherent demodulation is proposed for UWB systems. Closed form expressions are derived for the Bit Error Rate (BER) of the new demodulator. Results of simulations validate the derived theoretical BER performance of near-coherent detection.

1. Introduction

Regulations for UWB radio specify only the maximum value of psd and the minimum bandwidth over the assigned UWB frequency band that goes from 3.1 GHz to 10.6 GHz. Neither the type of carrier nor the modulation technique are defined. As shown in Fig. 1 the psd of Equivalent Isotropically Radiated Power (EIRP), measured with a resolution of 1 MHz, must be below -41.3 dBm [1].
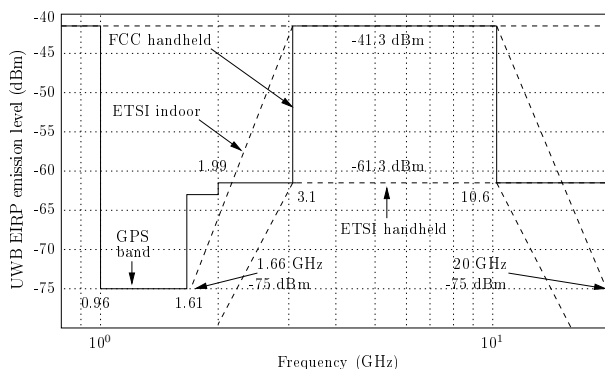

Figure 1: Emission limits for handheld and indoor UWB systems allowed by the European Technical Standards Institute (ETSI), dashed curve, and the Federal Communications Commission (FCC, USA), solid curve.

One-to-one recovery of UWB carriers is not feasible, consequently, a pure coherent UWB receiver cannot be built. On the other hand, noncoherent detectors offer a bad noise performance. As a trade-off, a new near-coherent detector configuration is proposed here where there is no need for an exact recovery of UWB carrier to perform detection.

2. Modulation schemes used in UWB radio

The waveforms used to carry digital information are ultra wideband signals in UWB radio with a 500-MHz minimum bandwidth. Fixed or chaotic carriers can be used to transmit information. The former is a deterministic signal while the latter is a continuously varying wavelet [2]. This paper considers the fixed waveform UWB radio.

2.1. Modulation using fixed waveform

In the simplest case, one bit information is carried by one fixed UWB wavelet. The structure of this UWB signal is shown in Fig. 2 where $g(t)$ denotes a fixed but arbitrary wavelet, used as carrier, in the pulse bin T_{bin}. Pulse
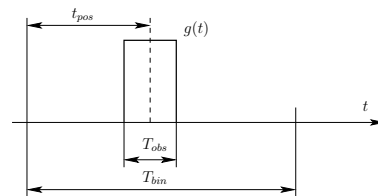

Figure 2: Waveform structure of UWB impulse radio.

bin determines the time elapsed between two consecutive wavelets, i.e. the symbol rate. Its role is to prevent intersymbol interference in a multipath channel. Observation time T_{obs} determines the interval during which the detector observes the received signal. The position t_{pos}, the amplitude and the sign of the wavelet may be varied in accordance with the digital information to be transmitted but the best noise performance is offered by an antipodal modulation scheme. Therefore, Pulse Polarity Modulation (PPoM) is considered here where the information is mapped into the sign of the radiated deterministic signal.

2.2. Deterministic wavelets used in UWB impulse radio

Since regulations specify only the psd mask and minimum bandwidth of UWB wavelet, there is a high degree of freedom in generating UWB waveforms.

Because of their excellent spectral properties the following UWB wavelets have been proposed: (i) Gaussian pulse [3], (ii) frequency-shifted bell-shaped Gaussian pulse [1], (iii) monocycle [3], and (iv) doublet pulse [3]. In this paper the bell-shaped Gaussian pulse is investigated

where the bandwidths are 2 GHz and 500 MHz. The only basis function takes the form

$$g(t) = \sqrt{\frac{2E_b}{\sqrt{\pi}u_b}} \exp\left(-\frac{t^2}{2u_B^2}\right)\cos(\omega_C t) = v(t)\cos(\omega_C t) \quad (1)$$

consequently, the elements of PPoM signal set are $s_{1,2} = \pm g(t)$. The carrier $f_C = \omega_C/2\pi$ is the UWB center frequency, E_b denotes the energy per bit, and u_B is a constant determined by the 10-dB bandwidth of UWB wavelet [1] and given by

$$u_B = \frac{1}{2\pi f_B \sqrt{\log_{10}e}}$$

where f_B, shown in Fig. 3, is the half of the desired RF bandwidth.
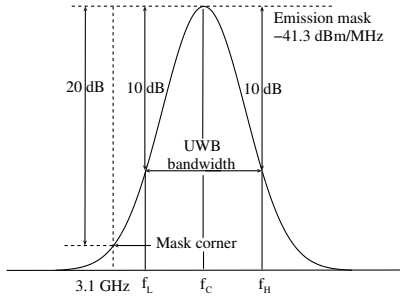

Figure 3: Definition of UWB bandwidth and constraints on UWB signal in the frequency domain.

Depending on their bandwidths (i) wideband, 2 GHz and (ii) narrowband, 500 MHz UWB systems are distinguished. The bell-shaped Gaussian wavelets are shown in the time domain for the wide- and narrowband UWB systems in Fig. 4. Although the duration of Gaussian wave-
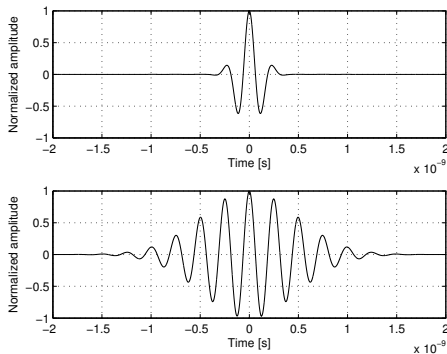

Figure 4: Bell-shaped Gaussian pulses with 2-GHz (upper trace) and 500-MHz (lower trace) bandwidths for f_C=4 GHz.

forms is infinite the power decreases rapidly as a function of time, consequently, the optimum duration of observation

time T_{obs} cannot be determined from the UWB wavelet, it is obtained from the noise performance of the PPoM modulation scheme. By definition, observation time assuring minimum BER is considered as T_{obs}.

To implement a near-coherent correlation receiver, a reference signal has to be generated. Because of their spectral shape, UWB carriers cannot be recovered. Instead, a noise-free reference signal approximating $g(t)$ over T_{obs} as close as possible should be found that may be recovered from the received UWB waveform by implementable circuitry.

As shown in Fig. 4, less than two cycles of carrier are transmitted in wideband UWB radio. The energy of such a signal is concentrated in the main lobe, therefore, the detection may be performed by windowing the received UWB waveform by a square-wave template signal [2]. This technique, referred to as template detection, is used if the energy of UWB signal is spread over a few carrier cycles.

In narrowband UWB radio, the UWB wavelet contains about 10 carrier cycles as shown in Fig. 4 for $f_C = 4$ GHz. In this case a sinusoidal signal recovered by a phase-locked loop (PLL) can be considered as a reference signal. The detection of narrowband UWB signal using a sinusoidal reference is referred to as near-coherent technique.

3. Near-coherent detection technique

In narrowband UWB impulse radio the transmitted signal contains enough cycles of the carrier to be recovered by a PLL, i.e. a sinusoidal reference $c(t)$ is used in the coherent correlation receiver. At the receiver a gated phase-locked loop (G-PLL) structure is used to recover $c(t)$.

The block diagram of near-coherent UWB detector proposed here for the narrowband UWB systems is shown in Fig. 5, where $r_m(t) = s(t) + n(t)$ is the received noisy sig-
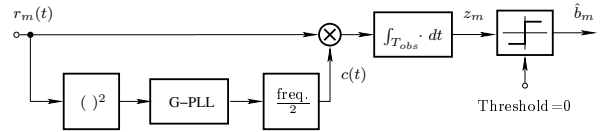

Figure 5: Block diagram of near-coherent UWB detector.

nal, $c(t)$ denotes the *quasi-recovered* carrier, z_m is the observation variable and $\hat{b}_m$ denotes the recovered digital information. The appellation *quasi-recovered* carrier refers to the main characteristic of near-coherent detection: although both the $r_m(t)$ and $c(t)$ have the same angle, the former has a Gaussian envelope while the latter is the output of a G-PLL therefore its envelope is constant. This mismatch in shape results in performance degradation. The information $\hat{b}_m$ can be recovered by correlating r_m with the sinusoidal reference $c(t)$.

Important advantage of near-coherent detection is that

$c(t)$ is a noiseless signal matched to the angle of $r_m(t)$

$$c(t) = \begin{cases} \sqrt{\dfrac{2}{T_{bin}}}\cos(\omega_C t), & \text{if } |t| < \dfrac{T_{obs}}{2} \\ 0, & \text{otherwise} \end{cases}$$

The received signal $r_m(t)$ is a modulated waveform. For the recovery of carrier first the modulation has to be eliminated that is performed by squaring the received signal. As shown in Fig. 6, the spectrum of a UWB signal carrying a random modulation has no carrier component. However squaring the modulated signal removes the modulation and generates a carrier component at $2f_C$

$$(\pm g(t))^2 = (\pm 1)^2 v^2(t)\cos^2(\omega_C t) = v^2(t)\frac{1 + \cos(2\omega_C t)}{2} \quad (2)$$

This $2f_C$ frequency component is selected by a G-PLL and then a frequency divider is used to generate the f_C frequency reference signal.
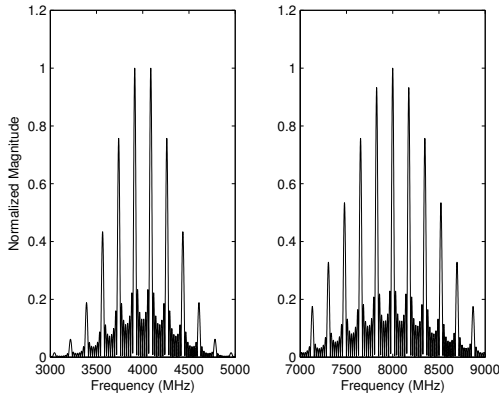

Figure 6: Spectrum of random series of bell-shaped Gaussian waveforms before (left plot) and after (right plot) squaring.

4. Noise performance of near-coherent detection

The model for investigation of the noise effects on the received signal is shown in Fig. 7.
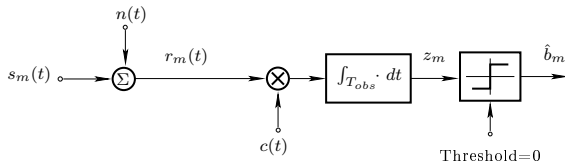

Figure 7: Model for investigation of the noise effects on the received signal.

Since the transmitted signal is corrupted by white Gaussian noise in an additive manner in the telecommunication channel, the observation signal, a random variable that appears at the output of the correlator can be expressed as

$$z_m = \int_0^{T_{obs}} s_m(t)c(t)\mathrm{dt} + \int_0^{T_{obs}} n(t)c(t)\mathrm{dt} \quad (3)$$

Recall that $c(t)$ is noiseless, consequently, $n(t)$ in (3) goes under a linear integral transformation. Therefore the distribution of the second term on RHS remains Gaussian and its expected value is zero [4].

The noise performance is determined from the observation variable. For antipodal modulation scheme using one basis function, the probability of bit error is given in the literature [5]

$$P_e = \frac{1}{2}\mathrm{erfc}\left(\frac{\mu_m}{\sqrt{2\sigma_n^2}}\right) \quad (4)$$

where μ_m is the expected value of observation variable and σ_n^2 is the power of noise, i.e. the variance of z_m. To get the BER for near-coherent UWB detection μ_m and σ_n^2 have to be found.

Since the second term on the RHS of (8) has zero mean, the mean of z_m is obtained as

$$\mu_m = \mathrm{E}\left[\int_0^{T_{obs}} s_m(t)c(t)\mathrm{dt}\right] = \sqrt{\frac{E_b\sqrt{\pi}u_B}{T_{bin}}}\mathrm{erf}\left(\frac{T_{obs}}{2u_B}\right) \quad (5)$$

where $E[.]$ is the expectation operator.

The channel noise $n(t)$ is modeled by a zero-mean stationary Gaussian process that has a uniform two-sided psd of $N_0/2$. The variance of the observation variable is obtained as [4]

$$\sigma_n^2 = \int_0^{T_{obs}}\int_0^{T_{obs}} R_n(t_1, t_2)c(t_1)c(t_2)dt_1 dt_2 \quad (6)$$

where $R_n(t_1, t_2)$ denotes the autocorrelation function of $n(t)$. Since $n(t)$ is stationary and white, its autocorrelation function is

$$R_n(t_1, t_2) = R_n(t_2 - t_1) = \frac{N_0}{2}\delta(t_2 - t_1) = \frac{N_0}{2}\delta(\tau) \quad (7)$$

Substituting (7) into (6), the variance of z_m is expressed

$$\begin{aligned}\sigma_n^2 &= \int_0^{T_{obs}}\int_0^{T_{obs}} \frac{N_0}{2}\delta(t - \tau)\frac{2}{T_{bin}}\cos(\omega_C t)\cos(\omega_C \tau)\,dt\,d\tau \\ &= \frac{N_0}{2}\frac{2}{T}\int_0^{T_{obs}}\cos^2(\omega_C t)\mathrm{dt} = \frac{N_0}{2}\frac{T_{obs}}{T_{bin}}\end{aligned} \quad (8)$$

Substituting (8) and (5) into (4), we get the BER for near-coherent detection

$$BER = \frac{1}{2}\mathrm{erfc}\left(\sqrt{\frac{\sqrt{\pi}u_B\left[\mathrm{erf}\left(\frac{T_{obs}}{2u_B}\right)\right]^2}{T_{obs}}}\sqrt{\frac{E_b}{N_0}}\right) \quad (9)$$

Equations (5) and (8) show that both the mean and variance of observation variable depend on the observation time. Consequently, the BER given by (9) also depends on T_{obs}, its value may be minimized by choosing the optimum value of T_{obs}.

Figure 8 shows the BER as a function of T_{obs}. Note, a global minimum exists at $T_{obs} = 1$ ns. This means that (9) can be minimized as a function of T_{obs}, its optimum value for our case is at $T_{obs} = 1$ ns.

Note, that any deviation from the optimum value of the observation time, results in a considerable performance degradation. For example, if the observation time is increased from 1 ns to 2 ns then BER also increases, from 10^{-8} to 10^{-6}.
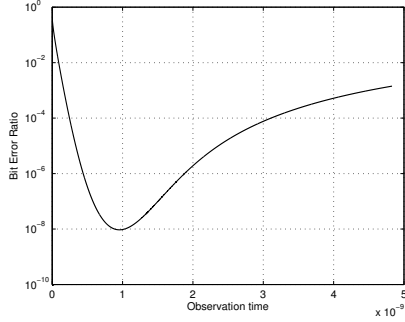

Figure 8: BER as a function of T_{obs} for $E_B/N_0 = 14$ dB.

The noise performance of the new near-coherent detector is shown in Fig. 9 for optimum and increased/decreased observation times. The BER of binary phase-shift keying (BPSK) is also shown for comparison. The transmitted carrier is not perfectly recovered in the proposed approach, instead, the recovered reference signal $c(t)$ is matched only in angle to the transmitted one. This mismatch error reduces the mean of z_m, therefore, the noise performance of near-coherent UWB detector always lags behind that of BPSK.

The theoretical results have been validated by computer simulations. The results of BER simulation are marked by crosses in Fig. 9.
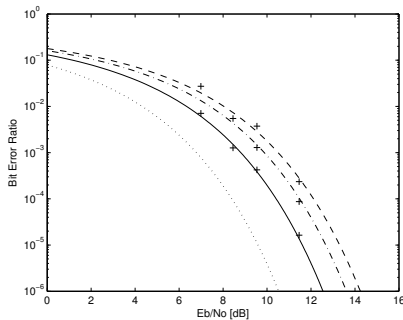

Figure 9: BER of BPSK (dotted curve), near-coherent detection for optimum T_{obs} (solid curve), for $2T_{obs}$ (dashed curve) and for $0.5T_{obs}$ (dash-dotted curve).

4.1. Effect of alignment error

Figure 2 shows that two kinds of timing errors appear in the near-coherent detector: (i) deviation from the ideal observation time duration and (ii) misalignment between observation time and the received UWB impulse. These errors are referred to as observation and alignment errors, respectively.

Effect of observation error has been studied in the previous section and plotted in Fig. 8.

Let the alignment error be quantified by $\Delta\tau_c$, for perfect alignment $\Delta\tau_c=0$. The alignment error has no influence on the variance of observation variable but it effects its mean value

$$\mu_m = \int_{-\frac{T_{obs}}{2}-\Delta\tau_c}^{\frac{T_{obs}}{2}-\Delta\tau_c} s_m(t)c(t)\mathrm{d}t = \sqrt{\frac{E_b\sqrt{\pi}u_B}{4T_{bin}}}\left[\mathrm{erf}\left(\frac{T_{obs}+2\Delta\tau_c}{2u_B}\right)+\right.$$
$$\left. + \;\; \mathrm{erf}\left(\frac{T_{obs}-2\Delta\tau_c}{2u_B}\right)\right] \quad (10)$$

From Equations (4) and (10) BER is obtained as

$$P_e = \frac{1}{2}\mathrm{erfc}\left(\sqrt{\frac{\sqrt{\pi}u_B\left[\mathrm{erf}\left(\frac{T_{obs}+2\Delta\tau_c}{2u_B}\right)+\mathrm{erf}\left(\frac{T_{obs}-2\Delta\tau_c}{2u_B}\right)\right]^2}{4T_{obs}}}\sqrt{\frac{E_b}{N_0}}\right) \quad (11)$$

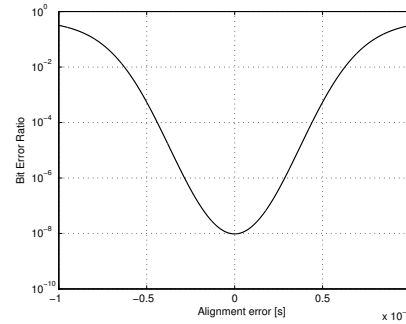The alignment error causes a noise performance degradation as shown by (11) and plotted in Fig. 10.

Figure 10: Effect of alignment error on the BER at $E_b/N_0=14$ dB.

5. Conclusions

A new near-coherent detection technique has been proposed for narrowband UWB impulse radio. A gated phase locked loop is used for the *quasi-recovery* of the basis function. An optimum T_{obs} has been found that offers the best noise performance. The sources of errors have been investigated. Simulation results validate the closed form expressions given for BER.

References

[1] K. Siwiak and D. McKeown, *Ultra-Wideband Radio Technology*, Wiley, Chichester, UK, 2004.

[2] G. Kolumbán and T. Krébesz, "UWB radio: A real chance for application of chaotic communications," in *Proc. NOLTA'06*, pp. 475–478, Bologna, Italy, September 11–14 2006.

[3] M. Ghavani, L. B. Michael, and R. Kohno, *Ultra-Wideband Signals & Systems in Communication Engineering*, Wiley, 2nd edition, 2006.

[4] J. S. Bendat and A. G. Piersol, *Measurement and Analysis of Random Data*, John Wiley & Sons, New York, 1966.

[5] S. Haykin, *Communication Systems*, Wiley, 3rd edition, 1994.